Cement and Concrete Research 38 (2008) 1169–1176

Contents lists available at ScienceDirect

Cement and Concrete Research

journal homepage: http://ees.elsevier.com/CEMCON/default.asp

Monitoring the setting of concrete containing blast-furnace slag by measuring the ultrasonic p-wave velocity

Nicolas Robeyst [a,*], Elke Gruyaert [a], Christian U. Grosse [b], Nele De Belie [a]

[a] Magnel Laboratory for Concrete Research, Ghent University, Department of Structural Engineering, Technologiepark Zwijnaarde 904, B-9052 Gent, Belgium
[b] Material Testing Institute, Stuttgart University, Department of Non-Destructive Testing and Monitoring, Pfaffenwaldring 4, D-70550 Stuttgart, Germany

ARTICLE INFO

Article history:
Received 12 November 2007
Accepted 11 April 2008

Keywords:
Ultrasonic
Calorimetry (A)
Fresh concrete (A)
Granulated blast-furnace slag (D)

ABSTRACT

Ultrasonic transmission measurements allow the continuous monitoring of the setting of both mortar and concrete samples, which is important to determine for instance the formwork removal time. However, aspects such as the cause of the low initial velocity, the relation between the velocity and the setting times and the effect of cement type or cement replacing additives are still under discussion. Therefore, different concrete compositions with blast-furnace slag were tested by traditional as well as ultrasonic measurements. The ultrasonic method gives a more complete picture of the setting. The change of ultrasonic velocity in time is sensitive to the differences in setting behaviour of the tested mixtures. The initial setting seems to correspond with the inflection point of the velocity-vs.-time graphs and the final setting with the point at which the velocity increase levels off.

1. Introduction

The development of methods to monitor the setting behaviour of fresh concrete benefits its practical application, since these techniques enable to determine the period that the concrete is workable. Moreover, a better comprehension of the setting process is also of fundamental importance for the study of the effect of admixtures and cement replacing additives on the stiffness development of concrete. Non-destructive ultrasonic measurements clearly offer advantages in this field, since they can be performed on both mortar and concrete, as opposed to the traditional methods such as the apparatus of Vicat (only on cement paste, EN 196-3) or the proctor needle test (only on mortar, ASTM C403). This study focuses on the application of the transmission method with compression waves (p-waves) which are less sensitive to difficulties with the sample-transducer contact than shear waves (s-waves) and allow a more accurate determination of the velocity through fresh concrete because of their higher signal-to-noise ratio. Both advantages are attributed to the ability of p-waves to propagate through fluids, in contrast to s-waves [1].

Much research has already been done on the ultrasonic wave transmission technique on fresh concrete by Reinhardt and Grosse [2], Voigt et al. [3] and Lee et al. [4] amongst others. However, aspects such as the origin of the low initial velocity and the relation between the velocity and the setting times are still under discussion. Therefore, in the first section of this paper, several theoretical descriptions of the ultrasonic wave velocity in suspensions and porous media are reviewed and applied to cementitious materials. The work of Sayers and Grenfell [5] on this subject is hereby extended to mortar and concrete. In the experimental part, different mortar and concrete compositions were tested by both traditional and ultrasonic measurements. These experiments were performed on mixtures with different blast-furnace cement types, in which the slag is ground together with the Portland clinker and gypsum in the production process of the cement itself (intergrinding). Additionally, also mixtures in which blast-furnace slag (BFS) was added as a separate component in the concrete composition (blending) were tested. In this way, the effect of mineral additives and different cement types on the ultrasonic measurements was investigated.

2. Theoretical background

The change that the velocity of an ultrasonic p-wave undergoes with time during setting and hardening of concrete, is already discussed in several papers [2,6,7]. In all velocity curves the following characteristic parts can be distinguished. The first part is the dormant period, characterised by a constant low velocity value. After this period, the velocity increases rapidly at first (second stage) and then more gradually (third stage) to finally reach an asymptotic value.

2.1. Initial wave velocity during the dormant period

Immediately after mixing, the p-wave velocity in cement pastes as well as in mortar and concrete mixes often reaches values lower than 600 m/s as reported by several researchers [4,8,9], while ultrasonic waves can propagate through water at a velocity of approximately 1500 m/s.

* Corresponding author. Tel.: +32 9 264 55 39; fax: +32 9 264 58 45.
E-mail address: Nicolas.Robeyst@UGent.be (N. Robeyst).

0008-8846/$ – see front matter © 2008 Elsevier Ltd. All rights reserved.
doi:10.1016/j.cemconres.2008.04.006

2.1.1. Cement paste

In fresh cement pastes, the poorly hydrated cement particles are initially isolated in the suspension. Although the pore water is fully connected, the ultrasonic velocity in this medium is low which can be attributed to the presence of air entrained during the mixing procedure since Chotard et al. [10] reported initial velocities of 1500 m/s in cement pastes in which the air bubbles were removed by underpressure. Moreover, the influence of entrapped air on the ultrasonic velocity in fresh mixtures can be demonstrated by the application of the theoretical model of Harker and Temple [11] for ultrasonic propagation in colloids. According to this model, the wave velocity in a suspension is given by

$$v_P^2 = \left[\left((1-\phi_s)\frac{1}{K_f} + \phi_s\frac{1}{K_s}\right)\cdot\left(\frac{\rho_f\cdot(\rho_s(1-\phi_s+\phi_s S)+\rho_f S(1-\phi_s))}{\rho_s(1-\phi_s)^2+\rho_f(S+\phi_s(1-\phi_s))}\right)\right]^{-1} \quad (1)$$

where ϕ_s is the solid volume fraction, K_f and K_s are the bulk moduli of the continuous (fluid) and discontinuous (solid) phases respectively and ρ_f and ρ_s are likewise the densities. The parameter S generally depends on the size and shape of the particles, the volume fraction ϕ_s and the continuous phase viscosity [12], but can be approximated by Eq. (2) for spherical particles in a fluid [13].

$$S = \frac{1}{2}\cdot\left(\frac{1+2\phi_s}{1-\phi_s}\right) \quad (2)$$

For cement particles, K_s is 105.2 GPa [14] and ρ_s is 3100 kg/m^3. When K_f is taken as the bulk modulus of water, namely 2.2 GPa, the initial velocity in a fresh cement paste with a w/c ratio of 0.5 (ϕ_s=0.392) is 1495 m/s. However, the compressibility of the continuous phase can be corrected for the presence of air assumed to be uniformly distributed.

$$\frac{1}{K_f} = \left(1-\frac{c_{air}}{1-\phi_s}\right)\cdot\frac{1}{K_{water}} + \frac{c_{air}}{1-\phi_s}\cdot\frac{1}{K_{air}} \quad (3)$$

In Eq. (3) c_{air} is the air content of the mixture and K_{air} is the bulk modulus of air, namely 142 kPa [15]. The change in wave velocity in the cement paste according to the air content is shown in Fig. 1, which resembles the results of Povey [16] in water–air systems. This calculation demonstrates that small percentages entrapped air (0.20–0.02%) can already reduce the velocity to values between 200 and 600 m/s.

2.1.2. Concrete and mortar

Fresh concrete and mortar can be considered as water-saturated media rather than suspension. In contrast to an early-age cement paste, they already have an elastic granular frame before the cement grains start to hydrate. Therefore, the theory developed by Biot [1] of

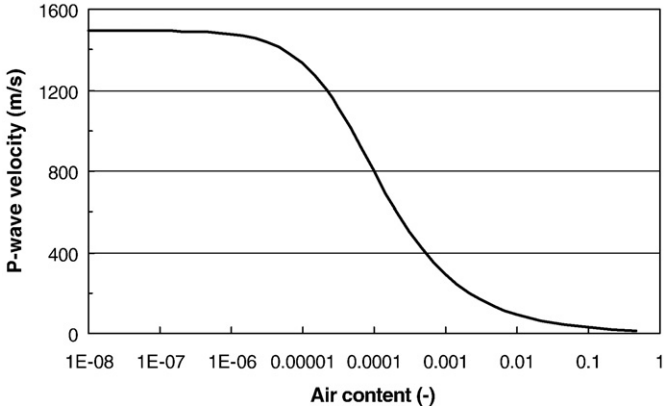

Fig. 1. The change in p-wave velocity in a cement paste (w/c=0.5) according to the air content as calculated with the theoretical model of Harker and Temple.

Table 1
Theoretical calculation of the initial wave velocity during the dormant period

Mixture	c_{air} (–)	n (=1−ϕ_s) (–)	K_f (MPa)	ρ_f (kg/m^3)	K (MPa)	G (MPa)	K_s (GPa)	ρ_s (kg/m^3)	v (m/s)
Mortar[a]	0	0.256	2200	1000	89	30	42.7	2750	1907
Mortar[a]	0.01	0.263	3.73	1000	89	30	42.7	2750	265
Concrete[b]	0	0.179	2200	1000	89	30	40.2	2713	2110
Concrete[b]	0.01	0.187	2.65	1000	89	30	40.2	2713	255

[a] Standard mortar according to EN 196-1.
[b] Concrete with w/c=0.5 and cement content 350 kg/m^3.

wave propagation in a fluid-saturated porous medium can be applied. According to this theory, an impulse applied to a two-phase medium splits into two waves of different velocity, termed fast and slow wave respectively. The slow wave is much more attenuated than the fast wave because of the shorter wavelength [17], and will not be discussed here. The velocity and the attenuation of the fast wave depend on the frequency regime defined by Biot based on the viscous skin depth δ given by Eq. (4).

$$\delta = \sqrt{\frac{\eta}{\pi\cdot\rho_f\cdot f}} \quad (4)$$

η is the viscosity of the fluid (10^{-3} Pa·s for water) and f is the frequency.

In the low frequency regime, δ is larger than the pore size of the medium and there is no movement of the fluid relative to the solid. In this case, the wave velocity can be written as

$$v_{P,low}^2 = \frac{K+\frac{4}{3}G+\frac{K_f(K_s-K)^2}{K_f(K_s-K)+K_s(K_s-K_f)n}}{(1-n)\rho_s+n\rho_f} \quad (5)$$

where K is the bulk modulus and G the shear modulus of the granular framework and n is the porosity.

In the high frequency regime, δ is smaller than the pore size of the medium and the tortuosity of the suspension gains importance. The ratio of the p-wave velocity at high and low frequencies can be calculated by Eq. (6) [15].

$$\frac{v_{P,high}}{v_{P,low}} = \sqrt{\frac{\left[n\alpha+n^2\left(\frac{\rho_s}{\rho_f}-2\right)-n^3\left(\frac{\rho_s}{\rho_f}-1\right)\right]\cdot\left[\frac{\rho_s}{\rho_f}(1-n)+n\right]}{\alpha\frac{\rho_s}{\rho_f}n(1-n)+n^2(\alpha-1)}} \quad (6)$$

The tortuosity α is approximately 1.9 for a sand frame [15] and 1.7 for gravel [18].

The centre frequency of the ultrasonic transducers used in this work is 0.5 MHz, which leads to a viscous skin depth of less than 1 μm compared with an initial pore size in the mortar of 30 μm [5] so the high frequency limit of the theory of Biot should be used. Taking into account an air content of 1%, the calculated solid volume fraction of a fresh standard mortar (EN 196-1) ϕ_s is 0.737. Thus, the porosity n amounts to 0.263 (n=1−ϕ_s) which is comparable with the porosity of dense sand. Therefore, K and G can be set to 89 MPa and 30 MPa respectively [19]. As the solid fraction in a standard mortar contains 77.8 vol.% sand (K_s=36.5 GPa, ρ_s=2650 kg/m^3 [20]) and 22.2 vol.% cement, K_s is 42.7 GPa and ρ_s is 2750 kg/m^3. With these values, the p-wave velocity in a fresh mortar mixture is 265 m/s, calculated with formulas (3), (5) and (6). Analogously, the velocity in a fresh concrete mixture amounts to 255 m/s (Table 1). It should be noted that these values are merely estimations under the important assumption that the entrapped air is uniformly distributed in the fresh mixture.

2.2. Increase of the wave velocity during hydration and final velocity

According to Voigt et al. [3], the very early increase in p-wave velocity is not attributed to setting, but to the formation of ettringite and to internal settling. Hydration products such as ettringite do not

create connected particles and have no or little influence on the stiffening process. However, they fill pore space as a result of which the porosity n in Eqs. (5) and (6) and the air content c_{air} in Eq. (3) decrease and the velocity increases. Internal settling due to gravity causes a better mechanical coupling of the particles without a real bond. As a result framework bulk modulus K and shear modulus G in Eq. (5) can increase and thus also the velocity increases. However, the largest velocity increase takes place during setting when the cement hydrates start to percolate and form complete pathways of connected particles for the ultrasonic pulse wave [9]. The mortar or concrete starts to acquire mechanical strength and can eventually be treated as homogeneous elastic solid material with an elastic Young's modulus E and a Poisson's ratio ν. The velocity can than be calculated with Eq. (7).

$$v_P = \sqrt{\frac{K + \frac{4}{3}G}{\rho}} = \sqrt{\frac{E \cdot (1-\nu)}{\rho \cdot (1-2\nu)(1+\nu)}} \tag{7}$$

For example, the velocity in concrete with elastic parameters E and ν equal to 36 GPa and 0.25 respectively is 4245 m/s.

3. Materials and methods

3.1. Mix design

Experiments on mixtures made with ordinary Portland cement (OPC) CEM I 52.5 were compared to mixtures in which 15%, 30%, 50%, 70% and 85% of the cement were replaced by BFS, added to the mixer separately. In addition, also compositions with OPC CEM I 42.5 and 4 different blast-furnace cement types (CEM III), in which BFS is interground with OPC during the production, were tested. According to EN 197-1, CEM III/A contains 36–65% BFS by mass, CEM III/B 66–80% and CEM III/C 81–95%. The chemical composition, the maximum theoretical hydration heat according to the mineralogical composition calculated with the formulas of Bogue and the specific surface area of the cement types and the BFS are given in Table 2.

Both mortar and concrete were tested. The standard mortar samples consisted of 1350 g standard sand, 450 g cement and 225 g water and were mixed according to EN 196-1. The concrete had a water/binder (w/b) ratio of 0.5 and the composition for 1 m^3 was:

Cement 350 kg
Water 175 kg
Sand 0/4 791 kg
Gravel 2/8 425 kg
Gravel 8/16 618 kg.

Table 2
Chemical composition (%), mineralogical composition according to the Bogue calculation (%), maximum hydration heat (J/g) and Blaine specific surface area (kg/m^3) of the cement and the blast-furnace slag

Cement type[a]	CEM I 52.5	BFS	CEM I 42.5	CEM III/A 42.5	CEM III/B 42.5	CEM III/A 32.5	CEM III/C 32.5
CaO	62.21	40.38	63.13	51.88	45.17	49.85	43.66
SiO_2	18.84	34.35	21.22	25.15	28.78	26.88	31.55
Al_2O_3	5.39	11.36	3.90	7.39	8.89	8.30	9.42
Fe_2O_3	3.79	0.48	5.05	2.32	1.55	2.01	0.83
MgO	0.86	7.57	0.89	4	5.80	4.22	4.22
SO_3	3.06	1.65	1.70	3.29	3.33	2.97	2.07
CO_2	0.72	0.25	0.39	1.17	1.83	1.16	0.97
Cl^-	0.04	0.013	0.01	0.04	0.04	0.04	0.22
C_3S	59.6	–	57.4	–	–	–	–
C_2S	9.1	–	17.6	–	–	–	–
C_3A	7.9	–	1.8	–	–	–	–
C_4AF	11.5	–	15.4	–	–	–	–
Hydration heat	465	–	431	–	–	–	–
Blaine SSA	370	400	315	485	450	345	317

[a] Terminology according to EN 197-1.

Table 3
Slump (mm) and air content (vol.%) of the mixtures with CEM I 52.5 and different replacement levels of blast-furnace slag and of the mixtures with different cement types

%BFS	0	15	30	50	70	85
Slump	130	60	120	80	70	50
Air content	2.5	2.7	2.9	2.1	1.9	1.4
Cement type	CEM I 42.5	CEM III/A 42.5	CEM III/B 42.5	CEM III/A 32.5	CEM III/C 32.5	
Slump	110	50	50	70	30	
Air content	2.7	2.1	1.8	2.0	1.4	

The repeatability value of the slump is 16 mm (EN 12350-2) and of the air content is 0.4% (EN 12350-7).

For each mixture the slump (EN 12350-2) and the air content (EN 12350-7) were determined and are summarized in Table 3.

3.2. Ultrasonic wave transmission measurements

The ultrasonic p-wave transmission measurements on the hardening mortar and concrete samples were performed with the FreshCon system developed at the University of Stuttgart. A detailed drawing of the sample cell is given by Reinhardt and Grosse [2]. Every 5 min, a pulse signal with a width of 2.5 μs was generated by the DAQ card of the FreshCon computer, of which the amplitude was increased by the amplifier (up to 800 V). The ultrasonic wave was then transmitted through the fresh concrete or mortar sample with the aid of a piezoelectric broadband transmitter. After traveling through the hardening sample, the signal was received by the ultrasonic receiver and sent back to the DAQ card. The onset of the received signal was detected manually during the first 2 to 3 h and then automatically with the Akaike Information Criterion (AIC) algorithm. More details about the FreshCon system and the AIC algorithm are described in previous publications [2,7]. During the setting and hardening process, the container was sealed with plastic film to limit concrete shrinkage resulting in decoupling of the sample and the container walls. All the tests were conducted at a room temperature of 20 °C.

Although the FreshCon system also measures the frequency content of the received ultrasonic signals, the focus will be on the velocity. To estimate the repeatability with which the velocity can be determined, 3 standard mixtures of the same composition were tested. The repeatability error amounted to 10% during the first hours and decreased to 1%. By modeling the measured velocity curves mathematically, smooth curves can be presented in the following paragraphs which make the comparison between the different curves clearer. Moreover, characteristic points (e.g. point of inflection) can be determined accurately. The graph of the velocity in time can be modeled using multi-logistic functions as presented in formula (8) [7,21].

$$v(t) = \sum_i \frac{v_i}{1 + e^{(t-t_i)/g_i}} + c \tag{8}$$

This formula superposes two or more logistic functions with different slopes (determined by parameter g_i), points of inflection t_i and asymptotic values v_i (Fig. 2). The logistic function typically describes quantities that grow exponentially at the outset after which the growth is gradually decelerated by feedback mechanisms, producing an S-shaped curve. The velocity graphs also follow this S-shape and were modeled as multi-logistic functions with an average root mean square error of calibration (RMSEC) of 28 m/s.

3.3. Determination of initial and final setting times

The setting behaviour was also monitored more traditionally with the penetration resistance test (ASTM C403) on the mortar fraction of

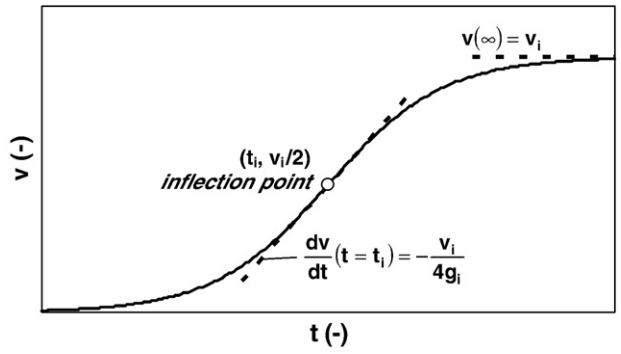

Fig. 2. Example curve demonstrating the different parameters of the logistic function.

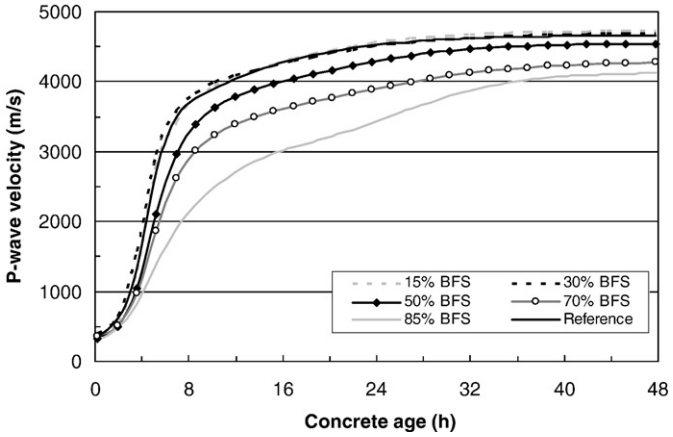

Fig. 3. Ultrasonic velocity vs. concrete age for concrete mixtures (w/c=0.5) in which an increasing percentage of the OPC (CEM I 52.5) was replaced by BFS.

the concrete mixtures. Since sieving the wet concrete mixture is not practical for concrete compositions with a w/b ratio of 0.5 and without plasticizers, the test was performed on an equivalent mortar mixture, calculated with the MBE method (Mortier de béton équivalent). In the MBE mixture, the gravel fraction is replaced by the amount of sand that has the same specific surface and the water amount is adjusted according to the difference in absorption between gravel and sand [22].

3.4. Semi-adiabatic calorimetric measurements

From every mixture, tested in the FreshCon system, a sample was put in a semi-adiabatic calorimeter (Langavant calorimeter) so ultrasonic and calorimetric measurements were conducted simultaneously. According to the semi-adiabatic method, the temperature rise of the hydrating sample in a heat-insulated flask is continuously measured. The cumulative heat production is then calculated with the following formula (EN 196-9):

$$Q = \frac{c}{m_c} \cdot \theta + \frac{1}{m_c} \sum_i \overline{\alpha_i} \cdot \overline{\theta_i} \cdot \Delta t_i \qquad (9)$$

where c is the thermal capacity of the setup, m_c the mass of cement, θ the temperature rise and $\overline{\alpha_i}$ and $\overline{\theta_i}$ the mean coefficient of heat loss and temperature rise of the test sample during period Δt_i. Since the mixing takes place outside the calorimeter, the first peak in the evolution of heat rate q is only partly registered and will therefore not be taken into account.

The temperature rise during the semi-adiabatic measurements can amount to 35 °C accelerating the hydration reactions, while the sample in the FreshCon container hydrates under almost isothermal conditions (the temperature increases less than 2 °C). To compare the results of the calorimeter with the ultrasonic measurements, the heat production rate will be shown as a function of the equivalent age at 20 °C, calculated with the maturity function according to the Arrhenius law. The activation energy was set to the value of OPC, namely 33.5 kJ/mol [23] for all mixtures. Although the activation energy of BFS is much higher, this difference was not taken into account because of the difficulties in separating the slag and the cement reaction.

4. Results and discussion

4.1. Ultrasonic p-wave velocity

The change of ultrasonic velocities in time for concrete mixes with different replacement percentages of BFS is presented in Fig. 3. The initial velocity ranges from 324 to 412 m/s, which is higher than the estimated value of 255 m/s mentioned above (Table 1). The smaller theoretical value of the velocity is probably due to the assumption that the entrapped air is uniformly distributed in the mixture, causing the bulk modulus of the continuous phase K_f to decrease very rapidly with small percentages of air. In reality, part of the air is entrapped locally (e.g. in corners of the sample or beneath larger aggregates) so K_f does not decrease equally over the whole sample. On the other hand, the determination of the signal onset time and thus wave velocity is less accurate during this early period (repeatability error of 10%) due to larger signal attenuation compared to a more hardened material. The dormant period, during which the velocity does not increase, is merely 2 to 3 h for all the mixes. However, as discussed above, the early increase of the p-wave velocity is rather caused by other factors than by setting of the cement. In a small experiment performed on a standard mortar mixture in which the cement was replaced by non-reactive quartz filler, the velocity increased from 240 to 264 m/s during the first 48 h due to internal settling. Since the effect of the latter seems to be limited, it can be hypothesized that mainly the formation of early hydration products such as ettringite influences the velocity in the beginning.

Thereafter, the actual setting takes place. Since the ultrasonic velocity is a measure for the stiffness of the hardening concrete sample, the stiffness seems to develop slower with increasing BFS content. This deceleration is attributed to the fact that the hydration of the BFS is not initiated until the lime liberated during the hydration of OPC provides the correct alkalinity [24,25]. In mixtures with little BFS (15% and 30%), the difference with the reference is restricted to approximately 1.7% which is little more than the repeatability error. The slower setting becomes clear at replacement levels of at least 50%. After approximately 24 h, the ultrasonic velocity of the concrete containing 85% BFS shows a second steep increase that might be caused by the reaction of the slag.

The p-wave velocity graphs, measured on the concrete samples with different types of blast-furnace cement are shown in Fig. 4. The

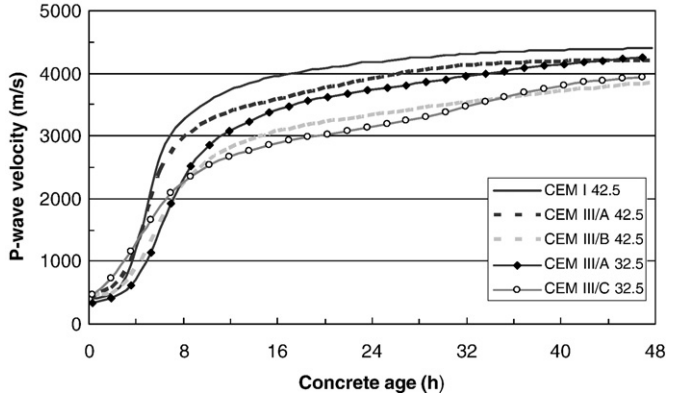

Fig. 4. Ultrasonic velocity vs. concrete age for concrete mixtures (w/c=0.5) with OPC and 4 different blast-furnace cement types.

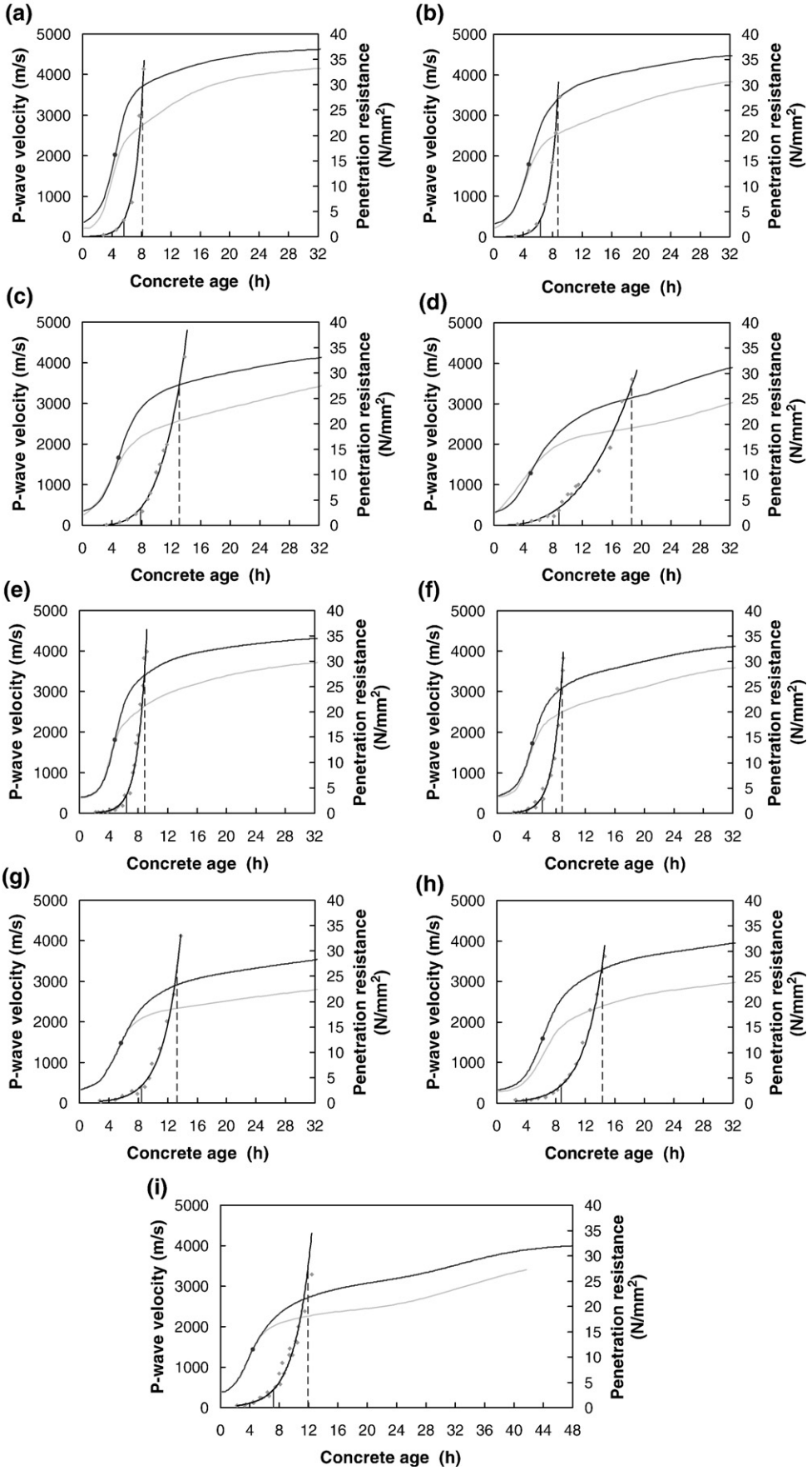

Fig. 5. Comparison between p-wave velocity and penetration resistance of the concrete mixtures with (a) CEM I 52.5, (b) CEM I 52.5+50% BFS, (c) CEM I 52.5+70% BFS, (d) CEM I 52.5+85% BFS, (e) CEM I 42.5, (f) CEM III/A 42.5, (g) CEM III/B 42.5, (h) CEM III/A 32.5 and (i) CEM III/C 32.5. The inflection point (·) and the initial (—) and final (- - -) setting times according to ASTM C403 are indicated. The p-wave velocity in the corresponding standard mortar is shown in grey.

same remarks about the low initial velocity and the short dormant period can be made for these mixtures. For cements of the strength class 42.5, the stiffness of the concrete sample seems to develop slower with increasing BFS content which is in agreement with the results mentioned above and shown in Fig. 3. However, for the strength class 32.5, during the first 12 h the velocity increases faster in the concrete made with CEM III/C than in the concrete with CEM III/A. This acceleration might be due to the higher chloride content of CEM III/C in comparison to CEM III/A (Table 2). According to Moranville-Regourd [26], chlorides act as accelerating agent. CEM III/A also contains a higher amount of gypsum (indicated by SO_3 content in Table 2), possibly leading to a slower hydration in the beginning. Thereafter, the velocity curve of the mixture with CEM III/C levels off, while the curve of the CEM III/A continues to increase. However, after approximately 26 h, the ultrasonic velocity of the concrete containing CEM III/C shows a second acceleration which was also noticed in the mixture with 85% BFS. In the last stage, the p-wave velocity reaches an asymptotic value which was not observed for some mixes within the measuring period of 48 h.

4.2. Comparison between ultrasonic velocity and penetration resistance

Fig. 5 gives the comparison between the ultrasonic measurements performed on concrete and on mortar and the penetration resistance tests performed on the equivalent mortar mixture. The initial and final setting times according to ASTM C403 are indicated and are determined by a penetration resistance of respectively 3.5 MPa (the concrete can no longer be vibrated) and 27.6 MPa (the concrete can carry measurable loads) [27].

For all the mixtures, the rise in ultrasonic p-wave velocity occurs sooner than the penetration resistance. As mentioned above, the ultrasonic velocity starts to increase when the first hydration products are formed, which fill up the pore space creating a denser structure and thus a higher bulk modulus (K). Jousset et al. [28] showed that the force, measured by the proctor needle mainly scales directly with the shear modulus (G) and hardly with the bulk modulus. Thus, an increase in bulk modulus will cause an increase in the p-wave velocity but not in penetration resistance. Only after some time, when the cement particles are connected, the shear modulus and thus the penetration resistance starts to develop [3]. This time corresponds with the inflection point of the velocity curve within a time window of 30 min for the investigated mixtures, which was also reported by Voigt et al. [3] for concrete with OPC. The initial setting indicated by ASTM C403 occurs later. For most of the mixes, the final setting corresponds quite well with the beginning of the third stage of the velocity curves, namely the slow increase in velocity. This correlation is presented in Fig. 6 in which the beginning of the slow velocity increase is indicated by the time when the derivative of the velocity curves has decreased to 20% of its maximum value. Concrete with a high BFS content (85% BFS and CEM III/C) deviates from this trend. For these mixtures, the evolution of the penetration resistance does not follow an exponential, but a power law indicating a slower setting process. Moreover, there is more deviation between the measured points and the regression curve in comparison with the results of the other mixtures and the second acceleration of the setting is not captured by the proctor needle.

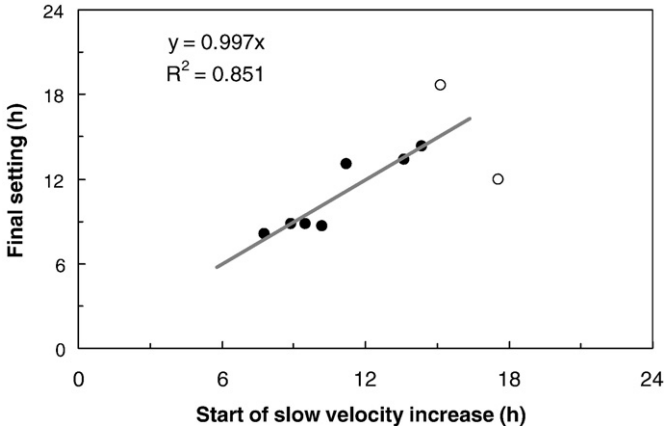

Fig. 6. Correlation between final setting (ASTM C403) and the start of the slow velocity increase (indicated by the age when the derivative of the velocity curve has decreased to 20% of its maximum value). The mixtures with a high BFS content (85% BFS and CEM III/C) deviate from the trend and are considered outliers (white dots).

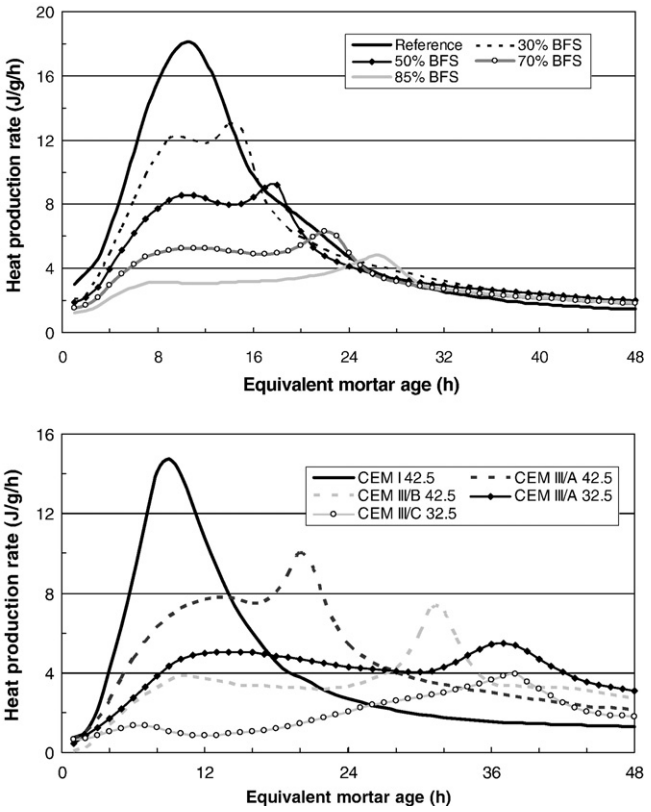

Fig. 7. The heat production rate q (Joule per g binder per h) vs. equivalent mortar age (20 °C) for standard mortars in which an increasing percentage of the Portland cement was replaced by blast-furnace slag (top) and for standard mortars with Portland cement and 4 different blast-furnace cement types (bottom) under semi-adiabatic conditions.

Fig. 5 also allows the comparison between the results of the ultrasonic measurements on the mortar (grey lines) and on the concrete (black lines) samples. The first hours after mixing, approximately until the inflection point in the velocity curve appears, the p-wave velocity in the concrete and in the mortar mixture changes analogously in time. The influence of the larger aggregates is rather small as long as the setting has not yet occurred [4]. This difference between concrete and mortar also indicates that the initial setting occurs around the time corresponding with the inflection point in the velocity graph.

As a final remark regarding the comparison between the ultrasonic velocity and setting times defined by the penetration resistance test, it should be noted that setting refers to the continuous transition from a fluid to a solid state. The terms initial and final setting as defined in standards such as ASTM C403 are used to describe arbitrarily chosen stages of setting in practice [24], while the ultrasonic method gives a more complete picture of the setting process.

4.3. Semi-adiabatic calorimetric measurements

Fig. 7 shows the heat production rate q under semi-adiabatic conditions, in function of the equivalent age at 20 °C. The quantity is

expressed by mass of total binder. As mentioned above, the first peak has been left out. The second peak, due to the rapid hydration of C_3S, appears earlier with increasing BFS content. The early hydration is stimulated by heterogeneous nucleation since the slag particles dispersed in the cement paste act as nucleation sites for the precipitation of hydration products [29].

For the mortar mixtures with BFS, also a third peak appears in the evolution of q. The more BFS is added, the more defined this peak becomes. The third peak can be due to the hydration of C_3A (the reaction of ettringite to monosulphate). According to Bensted [30] only a C_3A amount of more than 12% results in a visible third peak at 20 °C. However, according to Poppe and De Schutter [31] and Baert et al. [32] the reactions of C_3A in cement types with low C_3A content can be activated at 20 °C by respectively limestone filler and fly ash. In the case of BFS addition, the third peak is more likely attributed to the hydration of the BFS itself. The lime liberated during the hydration of C_3S (second peak) can indeed provide the correct alkalinity to initiate the slag reaction. Zou et al. [33] demonstrated with scanning electron microscopy that part of the BFS in blended cement already starts to react the first day after mixing. Moreover, the cumulative heat production Q amounts to almost 1200 J/g cement for the mixture with 85% BFS at 20 °C after 6 days, while the maximum theoretical heat release of the OPC used in this study is 465 J/g (Table 2). Therefore, it is more likely that also the BFS reacts the first days after mixing and contributes to the heat release. This additional hydration peak is more pronounced in the interground slag cement (Fig. 7, bottom) than in the blended BFS mixes (Fig. 7, top).

As mentioned above, to convert the age of the samples to the equivalent age at 20 °C, the activation energy was set to the value of OPC and the higher value of the BFS reaction was not taken into account. Consequently the second peak in the heat production rate will be located correctly, on the assumption that the activation energy of the OPC is not influenced by the addition of BFS. The third peak on the other hand will occur little too early.

4.4. Comparison between ultrasonic velocity and calorimetric measurements

With the semi-adiabatic calorimeter the heat production in time of the concrete or mortar sample is determined to monitor the hydration process, which is the overall chemical reaction of the cement and slag grains. Setting, on the other hand, refers to the mechanical evolution of the cement paste in the sample. However, since the shear strength is proportional to the amount of precipitated hydrates for a given w/c ratio, hydration and setting are closely related [34]. According to Pinto and Hover [35] final setting occurs when a specific level of microstructure development (degree of hydration) has occurred. Consequently, a comparison between ultrasonic velocity and calorimetric measurements is meaningful.

The second peak in the heat production rate occurs approximately 9 h after mixing for the OPC concrete. This age corresponds with the age at which the velocity graph levels off. The latter can be considered as the final setting, since setting occurs during the acceleratory period of the heat production [25]. The third hydration peak attributed to the reaction of the BFS, accounts for the largest part in the heat development of the mixes with high BFS content (85% BFS and CEM III/C) and explains the second acceleration of the ultrasonic velocity measurements. The formed slag hydration products can start to coagulate and accelerate the setting process that was already started with the coagulation of the cement hydration products.

As suggested by Herb [36] the ultrasonic velocity can be shown in function of the reaction degree r, calculated from the calorimetric measurements with Eq. (10).

$$r = \frac{Q}{Q_{max}} \tag{10}$$

where Q_{max} is the maximum cumulative heat measured after 7 days. After the dormant period, a bilinear relation between the ultrasonic velocity and the reaction degree can be seen for the reference mortar mixture in Fig. 8. According to Herb, the first straight line represents the setting and stiffening of the concrete or mortar sample, while the second one visualizes the hardening process. Consequently, the intersection would indicate the final setting. In case of the reference mixture, the intersection occurred at a reaction degree of 8.5%. However, in case of concrete mixture with OPC and a w/b ratio of 0.5, the model of Schindler shown in Eq. (11) predicts initial and final setting to occur at reaction degrees of 7.5% and 13% respectively [37] so the intersection is situated closer to the initial setting.

$$\begin{aligned} &\text{initial set}: \; r_i = 0.15 \cdot w/c \\ &\text{final set}: \; r_f = 0.26 \cdot w/c \end{aligned} \tag{11}$$

The reaction degree of 7.5% is reached 4.7 h after mixing, thus close to the point of inflection of the velocity curve (4.5 h after mixing). More likely, the final setting is indicated by the beginning of the second straight part of the graph.

5. Conclusions

The ultrasonic transmission method draws a more complete picture of the setting process than for example the penetration resistance method. The increase of the ultrasonic velocity during setting is generally retarded if more than 30% of the OPC is replaced by BFS. For the concrete containing high percentages of BFS (85% of the cementitious material or more), a second steep increase in the velocity graph attributed to the contribution of the slag hydration products to the setting, can be detected after approximately 24 h. This phenomenon is not captured by the penetration resistance method.

Initially the velocity merely reaches values between 300 and 420 m/s, which is theoretically proven to be attributed to air entrapped during the mixing procedure. The velocity starts to increase, when the first hydration products are formed, which have no or little influence on the stiffening process. Only after a time, when the cement particles are connected, also the penetration resistance starts to develop. Within a time window of 30 min, this age corresponds with the inflection point of the velocity curve and the point at which the velocity measurements in a concrete mixture starts to deviate from those in a mortar mixture. At this age a reaction degree of approximately 7.5% is reached, which is consistent with the prediction of initial setting according to Schindler.

The relation between the final setting and the velocity measurements is less clear. For most of the mixtures, it corresponds well with the beginning of the third stage of the velocity curves during which the velocity increases more gradually. However, this point cannot be determined as unambiguously as the point of inflection. Therefore, future research will be performed on extracting more information for instance from the ultrasonic wave energy.

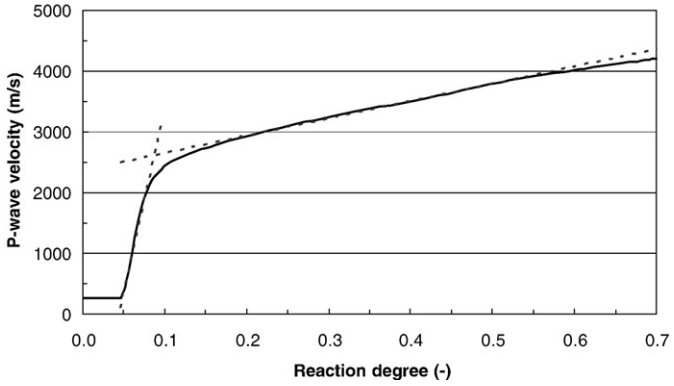

Fig. 8. Ultrasonic velocity vs. reaction degree for the standard mortar with CEM I 52.5.

Acknowledgement

As Research Assistants of the Research Foundation — Flanders (FWO — Vlaanderen), the authors Nicolas Robeyst and Elke Gruyaert want to thank the foundation for the financial support.

References

[1] M.A. Biot, Theory of propagation of elastic waves in a fluid-saturated porous solid, J. Acoust. Soc. Am. 28 (1956) 168–191.
[2] H.W. Reinhardt, C.U. Grosse, Continuous monitoring of setting and hardening of mortar and concrete, Constr. Build. Mater. 18 (3) (2004) 145–154.
[3] T. Voigt, C. Grosse, Z. Sun, S.P. Shah, H.W. Reinhardt, Comparison of ultrasonic wave transmission and reflection measurements with P- and S-waves on early age mortar and concrete, Mater. Struct. 38 (282) (2005) 729–738.
[4] H.K. Lee, K.M. Lee, Y.H. Kim, H. Yim, D.B. Bae, Ultrasonic in-situ monitoring of setting process of high-performance concrete, Cem. Concr. Res. 34 (4) (2004) 631–640.
[5] C.M. Sayers, R.L. Grenfell, Ultrasonic propagation through hydrating cements, Ultrasonics 31 (3) (1993) 147–153.
[6] N. De Belie, C.U. Grosse, J. Kurz, H.W. Reinhardt, Ultrasound monitoring of the influence of different accelerating admixtures and cement types for shotcrete on setting and hardening behaviour, Cem. Concr. Res. 35 (11) (2005) 2087–2094.
[7] C.U. Grosse, H.W. Reinhardt, M. Krüger, R. Beutel, Ultrasonic through-transmission techniques for quality control of concrete during setting and hardening, in: H.W. Reinhardt (Ed.), Advanced Testing of Fresh Cementitious Materials, Stuttgart, 2006, pp. 83–93.
[8] C.-L. Hwang, D.-H. Shen, The effects of blast-furnace slag and fly ash on the hydration of Portland cement, Cem. Concr. Res. 21 (4) (1991) 410–425.
[9] G. Ye, P. Lura, K. van Breugel, A.L.A. Fraaij, Study on the development of the microstructure in cement-based materials by means of numerical simulation and ultrasonic pulse velocity measurement, Cem. Concr. Compos. 26 (5) (2004) 491–497.
[10] T. Chotard, N. Gimet-Breart, A. Smith, D. Fargeot, J.P. Bonnet, C. Gault, Application of ultrasonic testing to describe the hydration of calcium aluminate cement at the early age, Cem. Concr. Res. 31 (3) (2001) 405–412.
[11] A.H. Harker, J.A.G. Temple, Velocity and attenuation of ultrasound in suspensions of particles in fluids, J. Phys. D, Appl. Phys. 21 (1988) 1576–1588.
[12] J.C. Austin, A.K. Holmes, J.S. Tebbutt, R.E. Challis, Ultrasonic wave propagation in colloid suspensions and emulsions: recent experimental results, Ultrasonics 34 (2–5) (1996) 369–374.
[13] T.E. Gomez Alvarez-Arenas, L. Elvira Segura, E. Riera Franco de Sarabia, Characterization of suspensions of particles in water by an ultrasonic resonant cell, Ultrasonics 39 (10) (2002) 715–727.
[14] K. Velez, S. Maximilien, D. Damidot, G. Fantozzi, F. Sorrentino, Determination by nanoindentation of elastic modulus and hardness of pure constituents of Portland cement clinker, Cem. Concr. Res. 31 (4) (2001) 555–561.
[15] M. Emerson, P. Foray, Laboratory P-wave measurements in dry and saturated sand, Acta Geotech. 1 (2006) 167–177.
[16] M.J.W. Povey, Ultrasonic Techniques for Fluid Characterization, Academic Press, San Diego, 1997.
[17] S. Jan Kowalski, Ultrasonic waves in diluted and densified suspensions, Ultrasonics 43 (2) (2004) 101–111.
[18] O. Umnova, K. Attenborough, H.-C. Shin, A. Cummings, Deduction of tortuosity and porosity from acoustic reflection and transmission measurements on thick samples of rigid-porous materials, Appl. Acoust. 66 (6) (2005) 607–624.
[19] M. Budhu, Soil Mechanics and Foundations, John Wiley & Sons, New York, 2000.
[20] T. Ahrens, Mineral Physics and Crystallography: a Handbook of Physical Constants, American Geophysical Union, Washington, 1995.
[21] N. Robeyst, E. Gruyaert, N. De Belie, Ultrasonic monitoring of setting and hardening behaviour of concrete and mortar with blast furnace slag cement, 12th International Congress on the Chemistry of Cement, Montréal, 2007.
[22] A. Schwartzentruber, C. Catherine, La méthode du mortier de béton équivalent (MBE) – Un nouvel outil d'aide à la formulation des bétons adjuvantés, Matér. Constr. 33 (2000) 475–482.
[23] G. De Schutter, Hydration and temperature development of concrete made with blast-furnace slag cement, Cem. Concr. Res. 29 (1) (1999) 143–149.
[24] A.M. Neville, Properties of Concrete, Longmen, Essex, 1995.
[25] H. Taylor, Cement Chemistry, Thomas Telford Publishing, London, 1990.
[26] M. Moranville-Regourd, Cements made from blastfurnace slag, in: P.C. Hewlett (Ed.), Lea's Chemistry of Cement and Concrete, Arnold, London, 1998, pp. 633–674.
[27] L.H. Tuthill, W.A. Cordon, Properties and uses of initially retarded concrete, Proc. — Am. Concr. Inst. 52 (2) (1955) 273–286.
[28] P. Jousset, D. Lootens, N. Roussel, R.J. Flatt, Rheology of penetrations tests I: theory and finite element simulations, 12th International Congress on the Chemistry of Cement, Montréal, 2007.
[29] J.I. Escalante-Garcia, J.H. Sharp, Effect of temperature on the hydration of the main clinker phases in Portland cements: part II, blended cements, Cem. Concr. Res. 28 (9) (1998) 1259–1274.
[30] J. Bensted, Some application of conduction calorimetry to cement hydration, Adv. Cem. Res. 1 (1) (1987) 35–44.
[31] A.-M. Poppe, G. De Schutter, Cement hydration in the presence of high filler contents, Cem. Concr. Res. 35 (12) (2005) 2290–2299.
[32] G. Baert, I. Van Driessche, S. Hoste, G. De Schutter, N. De Belie, Interaction between the pozzolanic reaction of fly ash and the hydration of cement, 12th International Congress on the Chemistry of Cement, Montréal, 2007.
[33] J. Zhou, G. Ye, K. Van Breugel, Hydration of Portland cement blended with blast furnace slag at early age, in: J. Marchand, B. Bissonnette, R. Gagné, M. Jolin, F. Paradis (Eds.), Second International Symposium on Advances in Concrete through Science and Engineering (Abstract Book, Full Paper on CD-ROM), Quebec, 2006, p. 371.
[34] A. Nonat, J.C. Mutin, From hydration to setting, in: A. Nonat, J.C. Mutin (Eds.), Hydration and Setting of Cements, Proc. of the International RILEM Workshop, Chapman & Hall, London, 1992, pp. 171–191.
[35] R.C.A. Pinto, K.C. Hover, Application of maturity approach to setting times, ACI Mater. J. 96 (6) (1999) 686–691.
[36] A. Herb, Indirekte Beobachtung des Erstarrens und Erhärtens von Zementleim, Mörtel und Beton mittels Schallwellenausbreitung, Universität Stuttgart, Stuttgart, 2003.
[37] A.K. Schindler, Concrete Hydration, Temperature Development and Setting at Early-ages, University of Texas, Austin, 2002.